Simpler and Cleaner Synthesis of Variously Capped Cobalt Nano-crystals Applied in Semi-hydrogenation of Alkynes

A. Sodreau[1], A. Vivien[1], A. Moisset[2], C. Salzemann[2], C. Petit[2,*] and M. Petit[1*]

[1]Sorbonne Université, CNRS, Institut Parisien de Chimie Moléculaire, UMR 8232, 4 place Jussieu, 75005 Paris, France.
[2]Sorbonne Université, MONARIS, UMR 8233, 4 place Jussieu, 75005 Paris, France.

Cobalt, Nanoparticles, Disproportionation, Hcp phase, Semi-hydrogenation.

ABSTRACT: Unlike the classical organometallic approach, we report here a synthetic pathway requiring no reducing sources or heating to produce homogenous hexagonal close packed cobalt nanocrystals (NCs). Involving a disproportionation process, this simple and fast (6 min) synthesis is performed at room temperature in presence of eco-friendly fatty alcohols to passivate Co NCs. Through a recycling step, the yield of Co NCs is improved and the waste generation is limited making this synthetic route cleaner. After an easy exchange of the capping ligands, we applied them as unsupported catalyst in the stereo-selective semi-hydrogenation of alkynes.

INTRODUCTION

Nowadays, the formation of well-defined nanoparticles (NPs) can be considered as common. Indeed, countless syntheses have been published over the past 20 years[1], increasing the morphological control and the originality of the nano-objects formed[2]. This new nanometric organization makes cobalt NPs appearing as promising materials with potential magnetic[3], electronic[4] and catalytic[5] applications. The chemical route highly contributed to this progress and allowed a high control on their structural homogeneity (shape, size, crystallinity), a crucial point to improve the performance of these objects[6]. This approach provided efficient ways to synthesis homogenous cobalt NPs using cobalt salts or organometallic complexes as starting material[7]. In **scheme 1**, we summarized remarkable strategies allowing to synthetize a wide range of cobalt nano-objects (spheres, rods, wires, disks…). The reverse micelles strategy generates nano-spheres at room temperature by a microemulsion of water in oil. The reduction of the cobalt salts was carried out with sodium borohydride, resulting in an undesirable formation of additional Co_2B NPs[8] **(scheme 1.a)**. The polyol method has the advantage of using the polyol itself as a solvent and reducing agent, but requires high temperature to induce the reduction process[9]. Well-defined nanorods or platelets can be obtained through a nucleating agent (Ru or Ir seeds) **(scheme 1.b)**. *Via* a hot injection of cobalt(0) complex Co_2CO_8, Alivisatos *et al.* induced its thermolysis and the formation of nanodisks in only few seconds. However, a mixture of crystalline phases was observed and pure hexagonal close packed (hcp) Co NPs remained difficult to isolate[10] **(scheme 1.c)**. A shape control was performed by Chaudret's group using $[Co(\eta^3\text{-}C_8H_{13})(\eta^4\text{-}C_8H_{12})]$ giving spheres and rods after respectively 3h and 48h (wires were also accessible with another ligand mixture in 48h). Nevertheless, 3 bars H_2 are required to reduce this cobalt(I) complex[11] **(scheme 1.d)**. More recently, the same group developed a new route involving $Co\{N(SiMe_3)_2\}_2$ to achieve polymorphismic nano-objects with variable crystalline structure, but a reductive atmosphere and 2 days at 150°C were required. A major drawback here, is the synthesis and the storage of the starting material[12] **(scheme 1.e)**.

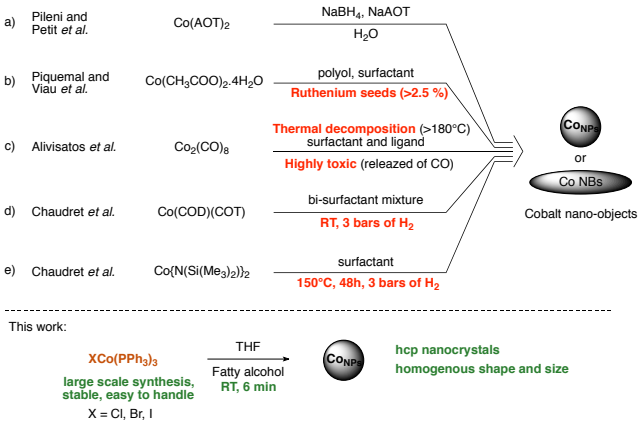

Scheme 1. Previous pathways to synthesize cobalt nano-objects (AOT = dioctyl sulfosuccinate).

These syntheses need specific synthetic conditions like high temperature, reductive atmosphere and/or additional reagents (reductants, nucleation seeds, etc.). Some of them also required long reaction time up to 2 days. In addition, some solvents and reagents involved in these syntheses can cause pollution and safety issues (toxic or explosive gases, high temperature, polluting waste, etc.). Consequently, development of a synthetic strategy presenting faster, cleaner and less energetic conditions appears as a key point to go further[13]. More generally, safer and eco-friendly reagents and conditions appear more and more mandatory.

Disproportionation process is a fairly old reaction described by Gadolin in 1788 on tin.[14] This redox pathway was used to synthesize gold[15] and copper[16] NPs. In the case of copper, fine

morphological control is obtained using thermodynamic or kinetic conditions[16b]. In 2016, we extended this pathway to cobalt by the formation of hcp cobalt nanospheres and nanorods in oleylamine at 190°C.[17]

In this context, it seems interesting to us to optimize this original process to synthesize cobalt nanoparticles under the mildest conditions. Herein, we report the synthesis of homogenous hcp-Co nanocrystals (NCs) at room temperature in just 6 minutes, implying a disproportionation pathway no reductive agents are necessary. Moreover, the capping of generated NPs is performed by bio-sourced fatty alcohol ligands, which is unusual for cobalt NPs but previously observed for other transition metal NPs.[18] In addition, through a recycling process, most of waste can be reused for the synthesis of the starting cobalt complex. Finally, we applied this cleaner pathway to synthesis cobalt nano-catalyst for semi-hydrogenation of alkynes.

RESULTS AND DISCUSSION

Recently, Nocera *et al.* were able to generate H_2 from HCl using $[ClNi(PPh_3)_3]$ as catalyst.[19] Interestingly, the proposal mechanism suggests as first catalytic step a disproportionation of this Ni(I) complex in THF at RT. In an older publication, Gosser described the formation of a "black magnetic powder" when $[ClCo(P(OPh)_3)_3]$ is dissolved in acetonitrile at 45°C and also concluded in a disproportionation process.[20] In these two examples, interactions between each complexes and its respective solvent are likely involved. Probably a solvent-phosphine exchange is capable of inducing this redox process. Indeed, MeCN and THF are known to be coordinated solvents, several examples present organometallic complexes coordinated by them.

Thus in our experiments, once $[ClCo(PPh_3)_3]$ was dissolved in THF a black precipitate stuck on the magnetic stirring bar and a blue supernatant were quickly observed at RT (**Table 1, entry 1**). This blue colour is characteristic of $[Cl_2Co(PPh_3)_2]$ complex suggesting a disproportionation process. Moreover, the ongoing monitoring of the colour of the solution allows the estimation of the end of the reaction. Initially brown, it quickly changed to black with emerald green reflects and when they turn night blue the reaction can be considered finished. It is assumed that this redox process generates $[Co(PPh_3)_4]$ and $[Cl_2Co(PPh_3)_2]$ in a 50:50 ratio from $[ClCo(PPh_3)_3]$. However, $[Co(PPh_3)_4]$ has never been isolated. Once generated, it rapidly degraded as metallic cobalt and free triphenylphosphine. In order to control the growth of these resulting cobalt nuclei, a wide range of ligands were tested (**Table 1**).

The first ligand we tested was oleylamine (OAm), a common fatty amine for capping NPs. With the addition of 5 equivalents (eq.) of OAm, only small polydispersed Co NPs were collected and the reaction time was greatly increased (**Table 1 *vs* entry 2**). This can be explained by a ligand exchange on the starting complex between triphenylphosphine and oleylamine, resulting in an inhibition of the THF effect. Then, other ligands were tested having closer coordination properties to THF. With ether ligands, the redox reaction occurred in 10 minutes or less. However, NPs isolated have a random shape and size (**Table 1, entries 3 to 6**). In presence of 5 equivalents of tridecanol, a fatty alcohol, NPs presenting homogenous shape and size can be easily collected in only 9 minutes (**Table 1, entry 8**). Variable amounts of tridecanol were tested to improve the reaction. With only 3 equivalents of tridecanol, the results were similar but the reaction time decreased to 6 minutes (**Table 1, entry 9**). Interestingly, no morphological changes were observed over the time (**Table 1, entry 9 vs entry 10**). Nevertheless, beyond 10 equivalents of tridecanol, the reaction time increased and the shape control is lost (**Table 1, entry 7**). Other alcohols have been tested: i) with a smaller alkyl chain such as octanol, the NPs formed are not well defined (**Table 1, entry 11**); ii) with longer alkyl chain such as octadecanol (stearyl alcohol), similar NPs were collected (**Table 1, entry 12**). Stearyl alcohol is interesting as a cheaper and innocuousness alternative to tridecanol. Among all these tests, 3 equivalents of tridecanol (or octadecanol) can be considered as the optimal conditions.

Table 1. Synthesis of nanoparticles by $[ClCo(PPh_3)_3]$ disproportionation in THF at room temperature.

Entry	Ligand	Amount	Time	Observations[a]
1	None	-	3 min	Black magnetic powder + blue supernatant
2	Oleylamine	5 eq.	24 h	NPs, d = 1.1 ± 0.6 nm
3	Diglyme	5 eq.	7 min	Polydisperse size NPs heterogeneous shape
4		1 eq.	3 min	
5	Dioctylether	5 eq.	8 min	Polydisperse size NPs heterogeneous shape
6		1 eq.	3 min	
7	Tridecanol	10 eq.	15 min	No homogenous shape
8		5 eq.	9 min	Spherical NPs
9		3 eq.	6 min	d = 8.7 ± 0.6 nm (7%)
10		3 eq.	30 min	Homogenous shape and size
11	Octanol	3 eq.	4 min	No homogenous shape
12	Octadecanol	3 eq.	4 min	Homogenous shape and size (d = 8.6 ± 0.5 nm)

[a]All TEM pictures are available in the supporting information (Table S1).

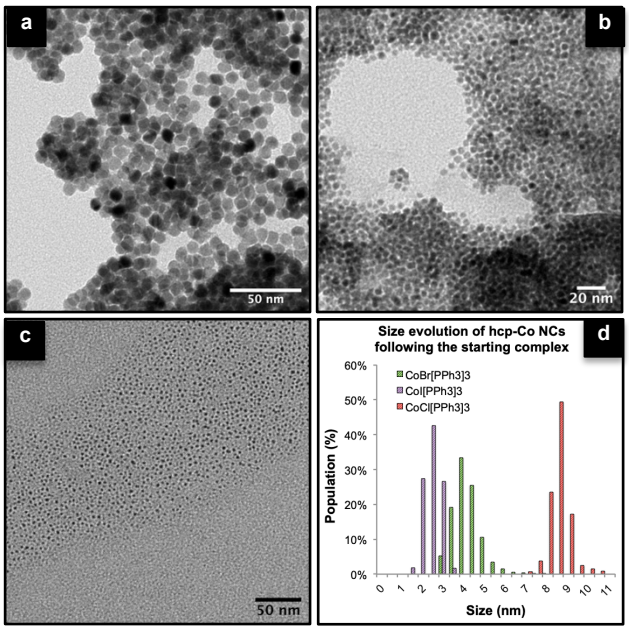

Figure 1. a) Synthesis of Co hcp-NCs from $[CoCl(PPh_3)_3]$, b) $[CoBr(PPh_3)_3]$, c) $[CoI(PPh_3)_3]$ complexes with 3 equivalents of tridecanol in THF in respectively 6, 12 and 45 min at room temperature. d) Evolution of the size of NPs by cobalt(I) complex used as starting material.

After ethanol treatment, the TEM pictures show spherical NPs with an average size of 8.7 ± 0.6 nm and a very small polydispersity (7%) (**Figure 1.a**). IR and SEM-EDX show mainly the presence of fatty alcohols, traces of chlorine and no triphenylphosphines (see Supporting Info). As we have shown in our previous approach,[21] the halide present on the starting complex has a significant importance on the kinetics of the disproportionation process. Indeed, with heavier halides derivatives, bromine and iodide, the reaction time increases up 12 min and 45 min respectively (**Figure 1.b-c**). This affects the size of NPs, which decrease according to the atomic number of the halide, from 8.7 ± 0.6 nm for chloride to 2.7 ± 0.4 nm for iodide (**Figure 1.d**).

Once isolated, the NPs can be re-dispersed in a solution of 20 eq. of OAm in toluene. Thereby, a ligand exchange between fatty alcohol and oleylamine was carried out. Oleylamine is a classic NPs surfactant known to generate 2D and 3D organization[1a]. After treatment, this exchange was monitored by TEM **(Figure 2)**. We also demonstrated that a partial or total ligand exchange could be realized with other chemical functions such as acid, phosphine or phosphine oxide (see Supporting Info).

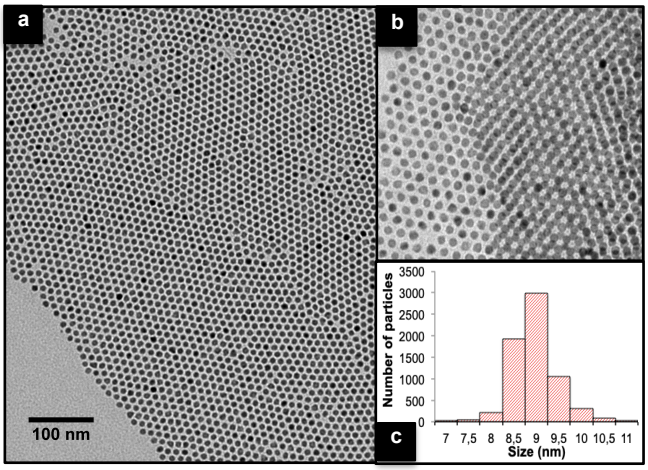

Figure 2. a) Co NPs after ligand exchange with oleylamine, b) Co NPs capped by OAm and organized 2D and 3D. c) Size distribution of Co NPs.

In order to fully characterize the structure of these 8.7 nm Co NCs, microscopic and macroscopic analyses were performed (**Figure 3**). The electron diffraction collected by TEM exhibits several rings showing the presence of a crystalline structure. After size measurement, the reticular distances corresponded to (100), (002), (101), (102), (110), (103), (200) and (112) crystalline plans of hcp crystalline phase (**Figure 3.d**). This phase was confirmed by High Resolution TEM (HRTEM) with the presence of similar distances found by Fourier transform corresponding to (100), (002) and (101) plans (**Figure 3.a-c**). X-Ray diffraction (XRD) analysis performed on NPs powder shows a set of fine peaks at 18.9°, 20.1°, 21.2°, 32.8°, 34.4°, 38.2° and 38.7° corresponding to hcp cobalt crystalline structure (**Figure 3.e**).

Scherrer's calculation was applied to the peak at 32.8° giving a crystallite size of approximately 8 nm matching with the size of NPs. All reticular distances and their corresponding plans of these analyses are summarized in **Table 2**. Nevertheless, broad peaks at 15°, 16.3° and 27° were also observed and correspond to Co_3O_4 crystalline structure. Scherrer's calculation applied to these peaks gives a crystallite size of smaller than 1 nm, likely resulting from an oxidized shell. This oxidation can be explained by the weakness of fatty alcohols as a chelating ligand. Interestingly, no oxidative layer is visible by microscopic analyses, so we cannot exclude a possible oxidation during the sample preparation.

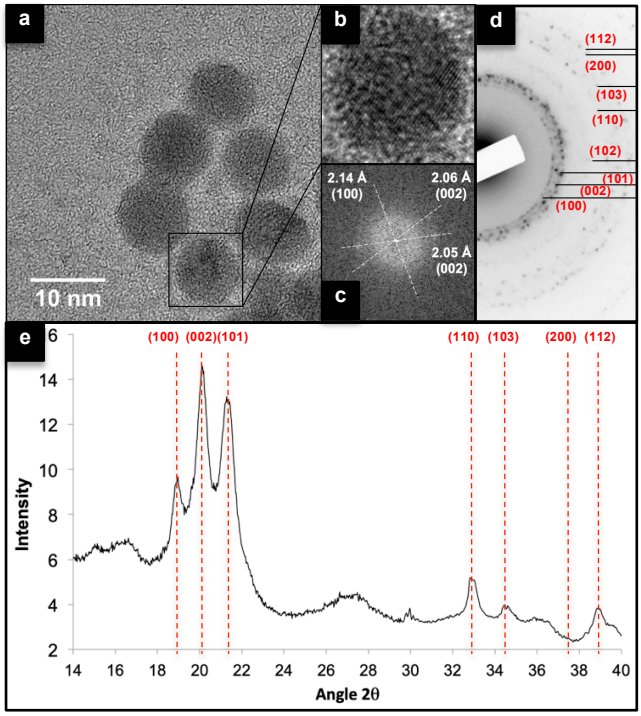

Figure 3. a) HRTEM pictures of the 8.7 nm Co NCs stabilized by fatty alcohol. b) Zoom on one isolated Co NCs, c) FT of this Co NCs. d) Electron diffraction from TEM of similar NPs. e) X-Ray diffraction of Co NCs powder.

Table 2. Theoretical reticular distances for bulk hcp Co, experimental reticular distances obtain by X-ray diffraction, TEM and HRTEM. All data are in Å.

h	k	l	dhkl (hcp) theorical	dhkl X-Ray diffraction	dhkl e- diff by TEM	dhkl HRTEM
1	0	0	2.171	2.16	2.21	2.14
0	0	2	2.025	2.03	2.07	2.05
1	0	1	1.916	1.92	1.93	1.91
1	0	2	1.485	-	1.54	-
1	1	0	1.254	1.25	1.27	-
1	0	3	1.150	1.19	1.17	-
2	0	0	1.086	1.08	1.09	-
1	1	2	1.067	1,07	1.06	-

In literature, Alivisatos *et al.*[10a] and Cheon *et al.*[22] have shown that the hot-injection of $Co_2(CO)_8$ at 180°C gives Co nanocrystals. After a rapid cooling and short reaction time (kinetic conditions) both of them observed a mixture of hcp-Co and ε-

Co. When the time of reaction increases to minutes (thermodynamic conditions) only a pure ε-Co phase is synthesized. However, under kinetic conditions, they specified that the mixture was mainly composed of hcp-Co, ε-Co was due to the too slow cooling of the medium. In our case, the disproportionation process allows a synthesis at RT in 6 minutes and only hcp-Co phase is observed which is consistent with kinetic conditions.

This structural organisation possesses a higher anisotropy improving the magnetic performance of these objects.[22] Therefore, Co NCs magnetic behaviour was monitored by vibrating-sample magnetometer (VSM). Their magnetization cycle was performed at 3 K and 300 K and we focus our attention on the coercity field (**Figure 4.a**). It decreased with the temperature from 0.17 T to 0.03 T respectively at 3 K and 300 K, but at both temperatures, an open hysteresis loop is clearly observed. Thus observations are consistent with a ferromagnetic behaviour as described by Zhang *et al.* with other hcp-cobalt NPs (0.16 T at 3 K and 0.05 T at 300 K).[23]

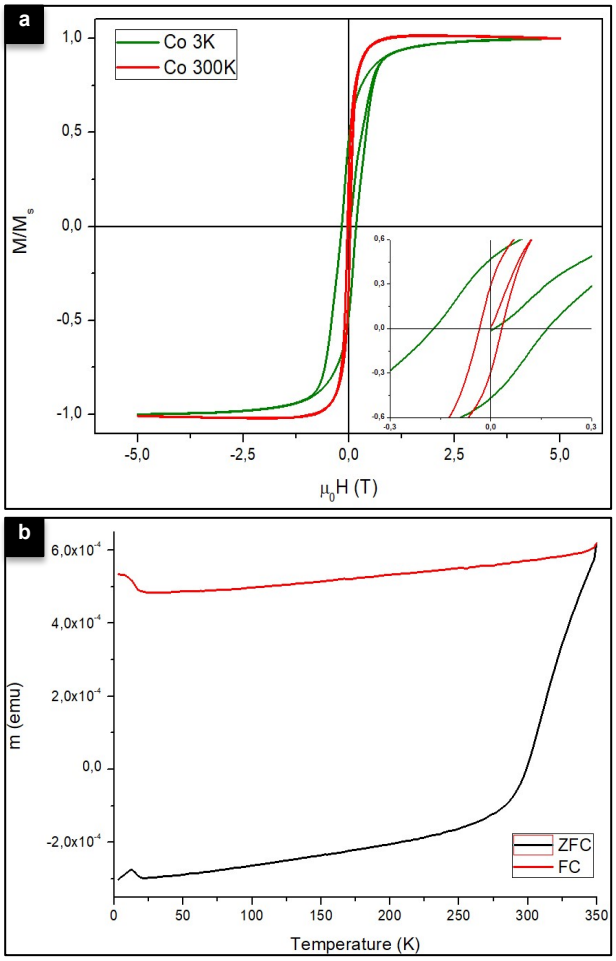

Figure 4. a) ZFC-FC curve obtained for 8.7 nm spherical Co NCs in solution with an EtOH quench.[23b] b) Magnetization curves at 3K and 300K of 8.7 nm spherical Co NCs in solution with an EtOH quench.

We also reported zero-field cooled / field cooled (ZFC/FC) measurement (**Figure 4.b**). First, a peak was observed on ZFC curve at 10 K. This may be due to traces of oxide previously mentioned after XRD analysis. Secondly, no overlap of ZFC and FC curves was observed below 350 K. Consequently, the blocking temperature T_B (transition temperature between superparamagnetic and ferromagnetic fields) was not reached at 350 K. Theoretically, T_B is estimated at 410 K for NPs with d ~ 8.7 nm (magnetic anisotropic constant of hcp cobalt = 4.1 x 10^5 J.m^{-3}) explaining the ferromagnetic behaviour observed at RT. Interestingly, 8 nm cobalt NPs synthesized by Legrand *et al*. with a fcc structure present a lower T_B at only 85 K, for non-isolated NPs.[24] Such an observation confirms the hcp structure of these NPs.

As mentioned, this redox pathway generates a maximum of 50% of $[Co(PPh_3)_4]$ induce an expected yield of 50%. This can be considered as a major drawback in the development of this synthetic route. Nevertheless, after calcination of stabilized Co NPs only 42 mol% of cobalt introduced is contained in the NPs. Moreover, after ethanol treatment, the NPs are easily separated from the solution of $[Cl_2Co(PPh_3)_2]$ and free triphenylphosphine which can be recycled in $[ClCo(PPh_3)_3]$ by addition of $NaBH_4$ with a yield of 76 %. Thus, based on recovered starting material the yield of the reaction is 86% **(Scheme 2)** and after two recycling runs the yield of isolated NPs increases up to 68%.

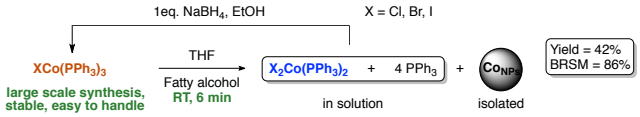

Scheme 2. Synthesis of NPs *via* a disproportionation pathway at RT and recyclability of cobalt(II) complex in starting material.

A recent publication estimated that a quarter of chemical transformations involve at least one hydrogenation step[25a]. In this context, NPs are more and more applied in catalytic hydrogenation, taking advantage of their large specific surface due to a high surface/volume ratio[25b]. Therefore, the development of Co NPs easily synthesized emerges as a promising pathway to access to hydrogenation catalyst. Recently, Beller's group published a selective semi-hydrogenation of alkynes using supported cobalt NPs as catalyst.[5a] Compared to the two others crystalline phases accessible for Co NPs (ε and fcc), the hcp-Co structure is acclaimed in catalysis,[26] for instance, experimental observations show that Fisher-Tropsch's reaction was better performed by hcp-cobalt catalyst.[27] Therefore, we focus our attention on the semi-hydrogenation of diphenylacetylene (DPA) using unsupported hcp-Co NPs as catalyst. The catalytic experiments were performed under H_2 pressure and heated in an autoclave. All different conditions tested are resumed in **table 3**.

Table 3. Unsupported Co NPs catalyzed semi-hydrogenation of diphenylacetylene.

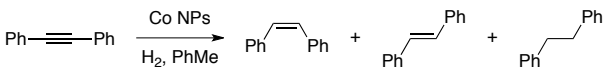

				Z		E	Alkane
Entry	**T/°C**	**t/h**	**H_2/bar**	**conv. (%)**	**Ratio E/Z[b]**		**Alkane (%)**
1[c]	120	16	30	99	1/99		17
2	120	16	20	99	5/95		15
3	120	16	10	90	1/99		7
4	120	1	30	99	4/96		3
5	RT	16	30	10	4/96		traces

6	RT	72	30	58	5/95	6

[a] Reaction conditions: 0.5 mmol of DPA in 2 mL of toluene containing 5 mol% of Co NPs capped by OAm. [b] Ratio of Z/E is determined by NMR. [c] Beller's hydrogenation conditions.

For all the conditions tested the *E*/*Z* ratio shows the *Z* isomer as major product with a high selectivity. The temperature of the reaction appears to be important. Indeed at 120°C after 16 hours 90% conversion can be reached whereas only 10% are observed at room temperature **(Table 3, Entry 1 vs 5)**. However, increasing the reaction time at room temperature to 72 hours allows to reach 58% conversion **(Table 3, Entry 6)**. It is noteworthy to mention that the overreduction to alkane is observed at 120°C when comparing 1h reaction with 16h reaction with no change of the selectivity **(Table 3, Entry 1 vs 4)**. Reducing the hydrogen pressure resulted in less alkane formation but lower conversion **(Table 3, Entries 1-3)**. We thus considered the conditions of the entry 1 for the extension to other alkynes because they give the highest conversion and ratio E/Z (in this case, the selectivity is higher than the one observed by Beller *et. al.*).

Table 4. Unsupported Co NPs catalyzed semi-hydrogenation of various alkynes.

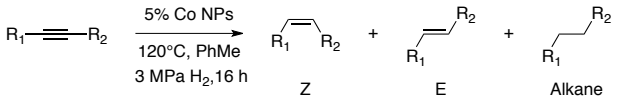

Entry	R1	R2	conv. (%)	Ratio E/Z	Alkane (%)
1	Ph	Ph	99	1/99	17
2	4-Br-Ph	4-Br-Ph	80	6/94	11
3	4-Bu-Ph	4-Bu-Ph	81	19/81	4
4	Ph	$SiMe_3$	24	17/83	-
5	Ph	CH_2OH	99	100/0	90
6	Ph	$CH(OH)CH_2$	88	100/0	68
7	Ph	CO_2Et	68	100/0	37
8	$C(CH_3)_2OH$	$C(CH_3)_2OH$	76	11/89	-

Similar selectivity is obtained with 4,4'-dibromoDPA, with good conversion. However, with electron donating groups as n-butyl in the *para* position, the formation of the E isomer is higher, with 80% conversion. Unsymmetrical alkynes can be also reduced. The presence of bulky group such as TMS is tolerated with similar selectivity but lower conversion is observed. Surprisingly, when the alkynes are bearing an alcohol or an ester substituent **(Table 4, Entries 5-7)** only the *E* isomer is observed together with the formation of important amount of alkane. A possible explanation can be that the presence of a chelating oxygen group at the propargyl position, may stick the molecule to the NPs and favor the overreduction. Indeed the none observed *Z* isomers seems to be readily reduced to the *E* one. However, the hydrogenation of the bulkier bis-isopropanol substituted acetylene shows this time the formation of the Z isomer as major product with no alkane **(Table 4, entry 8)**. The steric hindrance of this diol can justify that the molecule do not stay long on the surface and no overreduction is observed.

CONCLUSION

We describe here a room temperature expeditious synthesis of hcp cobalt NCs based on a disproportionation process. Mixing $[ClCo(PPh_3)_3]$ with fatty alcohol as a stabilizing ligand in THF carried out homogenous Co NPs in 6 minutes. Playing with the halide substituent on the complex, the NPs size can be varied from 2.7 to 8.7 nm. These Co NPs have been fully characterized by XRD, TEM, HRTEM and VSM and exhibit an hcp crystalline structure consistent with the synthetic conditions (kinetic conditions). Furthermore, initially at 50% the yield was improved to 77% by recycling by-products. Compared to previous syntheses published, this synthesis proposes a cleaner and less energetic pathway. A ligand exchange to oleylamine allowed a 2D and 3D organization and provides efficient Co NPs for catalytic semi-hydrogenation of alkynes. Catalytic tests show a high conversion and an interesting selectivity, with an inversion of ratio E/Z following the chelating properties of the substrate.

EXPERIMENTAL SECTION

General Procedure for the synthesis $X(PPh_3)_3Co$ complexes: On $CoX_2.6H_2O$, (40 mmoles) and triphenylphosphine (122 mmoles) were added 600 mL of degassed ethanol. The resulting heterogeneous solution was stirred vigorously at 60°C for 30 minutes environ to form in situ the complex $X_2(PPh_3)_2Co(II)$ as a bright blue powder. The mixture was then cool down to 30°C and sodium borohydride (34 mmoles) were added in 10 portions every 10 minutes. The color of the mixture changed from bright blue to dark brown. After 2 hours the brown precipitate was filtrated, washed sequentially with ethanol and diethyl ether and was finally dried under vaccum to give 25 g of the desired $[XCo(PPh_3)_3]$ complex with 76% yield.

Synthesis of Cobalt hcp-NCs: 132 mg of $[ClCo(PPh_3)_3]$ (0,15 mmol) was loaded in a screw-capped tube of 12 mL with a magnetic bar. In another tube, 90 mg of tridecanol (0,45 mmol) was dissolved in 6 mL of THF. Then, the solution of tridecanol was poured on $[ClCo(PPh_3)_3]$ under magnetic stirring. The solution color changed quickly from brown to black. After 6 minutes, about 15 mL of EtOH was added to the black solution and centrifuged at 2500 RPM for 5 min. A black powder was observed at bottom of tube with a blue supernatant. After elimination of the supernatant, the nanoparticles were dispersed in 2 mL of toluene and a drop was laid on a copper TEM grid to perform microscopic characterization. NPs from $[BrCo(PPh_3)_3]$ and $[ICo(PPh_3)_3]$ are prepare with the same procedure and amount than the one for $[ClCo(PPh_3)_3]$ precursor.

Recycling procedure: After 10 standard reactions, all supernatants were collected and transferred in schlenk tube. Then, under argon, 26 mg of $NaBH_4$ (0.9 eq.) were introduced in portion over 30 minutes under a vigorous stirring. After 4 hours at RT, the dark brown solid formed was filtrated and washed 3 times by EtOH and finally once by Et_2O. The solid was dried giving 490 mg of $[ClCo(PPh_3)_3]$.

Ligand exchange procedure: To a dispersed solution of NPs in toluene 20 eq. of oleylamine were added and mixed for 5 minutes. The excess of ligands was removed by a EtOH washing (20 mL).

Catalytic test: Under argon atmosphere, in a sealed tube was added 0.5 mmoles of the substrate with 2 mL of a toluene suspension containing 5 mol% of Co NPs passivated by oleylamine. Then the tube was introduced in an autoclave and filled with the desired pressure of hydrogen. The mixture was stirred and heated in an oil bath. At the end of the reaction the solution was filtered over silica and washed with pentane or ethyl acetate (depending on the polarity of the substrate). The solvent was removed under

reduced pressure to give the desired compound.

ASSOCIATED CONTENT

Supporting Information

Experimental procedures, microscopic analyses (TEM, SEM-EDX), size histograms, characterization of products resulting from alkynes catalysis and magnetic measurement information.
The Supporting Information is available free of charge on the ACS Publications website.

AUTHOR INFORMATION

Corresponding Author

* marc.petit@sorbonne-universite.fr
christophe.petit@sorbonne-universite.fr

ACKNOWLEDGMENT

This work was financially supported by CNRS, Sorbonne University and ANR program under reference NUMEN ANR-17-CE09-0037. The authors thank Sandra Casale (LRS, UMR 7197, Sorbonne Université, CNRS) for her help with the microscopic characterisation. We also gratefully acknowledge Mohamed Selmane (LCMCP, UMR 7574, Sorbonne Université, CNRS, Collège de France) for his contribution to the X-Ray Diffraction analysis. Céline Paris (MONARIS UMR 8233, Sorbonne Université, CNRS) is also acknowledged for her help with the infrared analysis.

REFERENCES

(1) a) Mourdikoudis, S.; Liz-Marzán, Luis M. Oleylamine in nanoparticle synthesis. *Chem. Mater.* **2013**, 25, 1465-1476. b) Sardar, R.; Funston, A.; Mulvaney, P.; Murray, R. Gold nanoparticles: past, present and future. *Langmuir* **2009**, 25, 13840-13851. c) Favier, I.; Pla, D.; Gómez, M. Palladium nanoparticles in polyols: synthesis, catalytic, couplings, and hydrogenations. *Chem. Rev.* **2020**, 120, 1146-1183.

(2) Nie, Z.; Petukhova, A.; Kumacheva, E. Properties and emerging applications of self-assembled structures made from inorganic nanoparticles. *Nat. Nanotechnol.* **2010**, *5*, 15–25.

(3) a) Hergt, R.; Dutz, S.; Müller, R.; Zeisberger, M. Magnetic particle hyperthermia: Nanoparticle magnetism and materials development for concer therapy. *J. Phys. Condens. Matter* **2006**, *18*, S2919–S2934. b) Mehdaoui, B.; Meffre, A.; Carrey, J.; Lachaize, S.; Lacroix, L-M.; Gougeon, M.; Chaudret, B.; Respaud, M. Optimal Size of Nanoparticles for Magnetic Hyperthermia: A Combined Theoretical and Experimental Study. *Adv. Funct. Mater.* **2011**, 21, 4573–4581.

(4) a) Krishnan, K. M.; Pakhomov, A. B.; Bao, Y.; Blomqvist, P.; Chun, Y.; Gonzales, M.; Griffin, K.; Ji, X.; Roberts, B. K. Nanomagnetism and spin electronics: materials, microstructure and novel properties. *J. Mater. Sci.* **2006**, *41*, 793–815. b) Sun, C.; Lee, J. S. H.; Zhang, M. Magnetic nanoparticles in MR imaging and drug delivery**.** *Adv. Drug Deliv. Rev.* **2008**, *60*, 1252–1265. c) Frey, N. A.; Peng, S.; Cheng, K.; Sun, S. Magnetic nanoparticles: synthesis, functionalization, and applications in bioimaging and magnetic energy storage. *Chem. Soc. Rev.* **2009**, *38*, 2532–2542. d) Reiss, G.; Hütten, A. Applications beyond data storage**.** *Nat. Mater.* **2005**, 4, 725–726.

(5) a) Chen, F.; Kreyenchulte, C.; Radnik, J.; Lund, K.; Surkus, E.; Junge, K.; Beller, M. Selective semihydrogenation of alkynes with N-graphitic-modified cobalt nanoparticles supported on silica *ACS. Catal.* **2017**, *7*, 1526–1532. b) Jagadeesh, R.; Murugesan, K.; Alshammari, A.; Neumann, H.; Pohl, M-M.; Beller, M. MOF-derived cobalt nanoparticles catalyze a general synthesis of amines. *Science*. **2007**, 358, 326–332. c) Harmel, J.; Peres, L.; Estrader, M.; Berliet, A.; Maury, S.; Fécant, A.; Chaudret, B.; Serp, P;. Soulantica, K. hcp-Co Nanowires Growth on Metallic Foams as Catalyst for Fisher-Tropch Synthesis, *Angew. Chem. Int. Ed.* **2018**, 57, 10579-10583.

(6) a) Li, Y.; Boone, E.; El-Sayed, M. Size Effects of PVP−Pd Nanoparticles on the Catalytic Suzuki Reactions in Aqueous Solution. *Langmuir*, **2002**, 18, 4921–4925. b) Wilson, O.; Knecht, M.; Garcia-Martinez, J.; Crooks, R. Effect of Pd Nanoparticle Size on the Catalytic Hydrogenation of Allyl Alcohol. *J. Am. Chem. Soc.* **2006**, 128, 4510–4511. c) Ranganath, K.; Glorius, F. Superparamagnetic nanoparticles for asymmetric catalysis—a perfect match. *Catal. Sci. Technol.* **2011**, 1, 13–22.

(7) Cormary, B.; Dumestre, F.; Liakakos, N.; Soulantca, K.; Chaudret, B. Organometallic precursors of nano-objects, a critical view. *Dalt. Trans.* **2013**, *42*, 12546–12553.

(8) a) Petit, C.; Pileni, M. P. Nanosize cobalt boride particles: Control of the size and properties. *JMMM*. **1997**, 166, 82–90. b) Petit, C.; Taleb A.; and Pileni, M.-P.; Self -Organization of Magnetic Nanosized Cobalt Particles, *Adv. Mat*., **1998** , 10, 259-261.

(9) a) Fievet, F.; Lagier, J. P.; Blin, B.; Beaudoin, B.; Figlarz, M. Homogeneous and heterogeneous nucleations in the polyol process for the preparation of micron and submicron size metal particles . *Solid State Ionics* **1989**, *32–33*, 198–205. b) Ramamoorthy, R.; Viola, A.; Grindi, B.; Peron, J.; Gatel, C.; Hytch, M.; Arenal, R.; Sicard, L.; Giraud, M.; Piquemal, J-Y.; Viau, G. One-pot seed-mediated growth of Co nanoparticles by the polyol process: unraveling the heterogeneous nucleation. *Nano. Lett.* **2019**, 19, 9160-9169.

(10) a) Puntes, V.; Zanchet, D.; Erdonmez, C.; Alivisatos, P. Synthesis of hcp-Co Nanodisks**.** *J. Am. Chem. Soc.* **2002**, 124, 12874–12880. b) Puntes, V.; Krishnan, K. ; Alivisatos, P. Colloidal Nanocrystal Shape and Size Control: The Case of Cobalt. *Science*. **2001**, 291, 2115–2117. c) Bao, Y.; An, W.; Turner, C.; Krishnan, K. M. The Critical Role of Surfactants in the Growth of Cobalt Nanoparticles. *Langmuir* **2010**, *26*, 478–483.

(11) Dumestre, F.; Chaudret, B.; Amiens, C.; Fromen, M. C.; Casanove, M. J.; Renaud, P.; Zurcher, P. Shape Control of Thermodynamically Stable Cobalt Nanorods through Organometallic Chemistry. *Angew. Chem. Int. Ed.* **2002**, *41*, 4286–4289.

(12) Liakakos, N.; Cormary, B.; Li, X.; Lecante, P.; Respaud, M.; Maron, L.; Falqui, A.; Genovese, A.; Vendier, L.; Koïnis, S.; Chaudret, B.; Soulantica, K. The Big Impact of a Small Detail: Cobalt Nanocrystal Polymorphism as a Result of Precursor Addition Rate during Stock Solution Preparation. *J. Am. Chem. Soc.* **2012**, 134, 17922–17931.

(13) Hebbalalu, D.; Lalley, J.; Nadagouda, M.; Varma, R. Greener techniques for the synthesis of silver nanoparticles using plant extracts, enzymes, bacteria, biodegradable polymers and microwaves. *ACS Sustainable Chem. Eng.* **2013**, 1, 703-712.

(14) Gadolin, J. K. Sv. Vet. Acad. Handle. **1788**, 186–197.

(15) Bergamini, G.; Ceroni, P.; Balzani, V.; Gingras, M.; Raimundo, J-M.; Morandi, V.; Merli, P. Synthesis of small gold nanoparticles: Au(I) disproportionation catalysed by a persulfurated coronene dendrimer. *Chem. Comm.* **2007**, 4167-4169.

(16) a) Guo, H.; Chen, Y.; Cortie, M. B.; Liu, X.; Xie, Q.; Wang, X.; Peng, D. L. Shape-Selective Formation of Monodisperse Copper Nanospheres and Nanocubes via Disproportionation Reaction Route and Their Optical Properties. J. Phys. Chem. C 2014, 118, 9801−9808. b) Strach, M.; Mantella, V.; Pankhurst, J.; Iyengar, P.; Loiudice, A.; Das, S.; Corminboeuf, C.; van Beek, W.; Buonsanti, R. Insights into reaction intermediates to predict synthesis pathways for shape-controlled metal nanocrystals. *J. Am. Chem. Soc.*, **2019**, 16312-16322.

(17) Meziane, L.; Salzemann, C.; Aubert, C.; Gérard, H.; Petit, C.; Petit, M. Hcp cobalt nanocrystals with high magnetic anisotropy prepared by easy one-pot synthesis. *Nanoscale* **2016**, *8*, 18640–18645.

(18) a) Pelzer, K.; Vidoni, O.; Philippot, K.; Chaudret. B.; Collière, V. Organometallic synthesis of size-controlled polycristalline ruthenium nanoparticles in presence of alcohols. *Adv. Funct. Mater.* **2003**, 13, 118. b) Ramírez-Meneses, E.; Philippot, K.; Domínguez-Crespo, M. A.; Ibrahim, M.; Betancourt, I.; Torres-Huerta, A. M.; Ezeta-Mejia, A. Synthesis of Rh nanoparticles in alcohols: magnetic and electrocatalytic properties. *J. Mater. Sci.* **2018**, 53, 8933.

(19) Hwang, S.; Powers, D.; Maher, A.; Nocera, D. Tandem redox mediator/Ni(ii) trihalide complex photocycle for hydrogen evolution from HCl. *Chem. Sci.* **2015**, 6, 917–922.

(20) Gosser, L. W. Synthesis and properties of cobalt(I) compounds. 5. Properties of tris(triphenyl phosphite)cobalt(I) halides**.** *Inorg. Chem.* **1977**, 430–434.

(21) Vivien, A.; Guillaumont, M.; Meziane, L.; Salzemann, C.; Aubert, C.; Halbert, S.; Gérard, H.; Petit, M.; Petit, C. Role of Oleylamine Revisited: An Original Disproportionation Route to Monodispersed Cobalt and Nickel Nanocrystals. *Chem. Mater.* **2019**, *31*, 960–968.

(22) Park, J-I.; Kang, N-J.;. Jun, Y-W.; Oh, S.; Ri, H-C.; Cheon, J. Superlattice and Magnetism Directed by the Size and Shape of Nanocrystals**.** *Chem. Phys. Chem.* **2002**, 6, 543–547.

(23) Zhang, Z.; Chen, X.; Zhang, X.; Shi, C. Synthesis and magnetic properties of nickel and cobalt nanoparticles obtained in DMF solution. *Solid State Communications.* **2006**, 139, 403–406.

(24) Legrand, J.; Petit, C.; Bazin, D.; Pileni, M.P. Collective effect on magnetic properties of 2D superlattices of nanosized cobalt particles. *Applied Surface Science*. **2000**, 164, 186–192.

(25) a) Zhang, L.; Zhou, M.; Wang, A.; Zhang, T. Selective hydrogenation over supported metal catalysts: from nanoparticles to simple atoms. *Chem. Rev.* **2020**, 120, 683-733. b) Asensio, J.; Bouzouita, D.; van Leeuwen, P.; Chaudret, B. σ-H–H, σ-C–H, and σ-Si–H bond activation catalysed by metal nanoparticles. *Chem. Rev.* **2020**, 120, 1042-1084.

(26) de la Peña O'Shea, V.; de la Piscina, P.; Homs, N.; Aromí, G.; Fierro, J. Development of hexagonal closed-packed cobalt nanoparticles stable at high temperature, *Chem. Mater.* **2009**, 21, 5637-5643.

(27) de la Peña O'Shea, V.; Campos-Martín, J.; Fierro, J. Strong enhancement of the fischer-tropsch synthesis on a Co/SiO_2 catalyst activate in syngas mixture. *Cat. Comm.* **2004**, 5, 635-638.

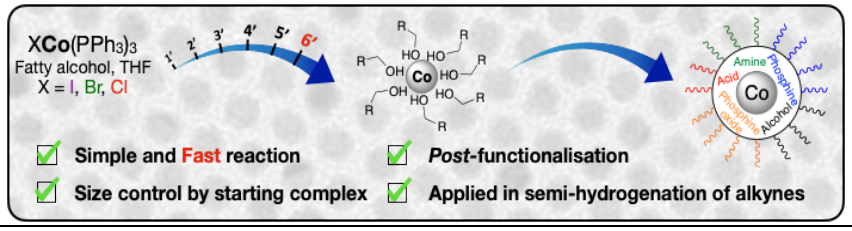
XCo(PPh3)3
Fatty alcohol, THF
X = I, Br, Cl
1'
2'
3'
4'
5'
6'
Co
Amine
Phosphine
Acid
Phosphine oxide
Alcohol
Simple and Fast reaction
Size control by starting complex
Post-functionalisation
Applied in semi-hydrogenation of alkynes